Jacek SOSNOWSKI

ANALYSIS OF THE INFLUENCE OF BENDING STRAIN ON THE CURRENT-VOLTAGE CHARACTERISTICS OF HTc SUPERCONDUCTING TAPES

ABSTRACT *In this paper the influence of the bending strain inherent in superconducting magnet windings on the current-voltage characteristics and the critical current of HTc superconducting tapes is investigated. Theoretical analysis of this effect is presented, which is in qualitative agreement with experimental research carried out on first generation superconducting tapes. The influence of the shape of the rupture probability function, which describes micro-crack formation, on the current-voltage characteristics is also considered.*

Keywords: *HTc superconducting tapes, bending strain, current-voltage characteristics*
DOI: 10.5604/01.3001.0010.0036

1. INTRODUCTION

High temperature oxide superconductors are very promising materials for use in electrical engineering [1-2]. The rapid progress in achieving higher critical temperatures, already as high as 203 K [3] in sulfur and selenium hydride, has given new impetus to work on using these materials in a new generation of devices containing superconducting windings. During the manufacture of coils, superconducting tape is bent, a process which leads to an increase in the strain on the tape and ultimately to the creation of micro-cracks influencing the electric current transport process. This paper is devoted to an analysis of this problem.

prof. Jacek SOSNOWSKI, Ph.D., D.Sc.
e-mail: j.sosnowski@iel.waw.pl

Electrotechnical Institute,
M. Pożaryskiego 28, 04-703 Warsaw, Poland

1. EXPERIMENTAL RESULTS

With the aim of counterchecking the theoretical model and verifying the real technical importance of this issue, experimental investigations of the influence of bending strain on the critical current of superconducting tapes have been carried out. The results of measurements taken at liquid nitrogen temperature of the current-voltage characteristics of Bi-2223 HTc superconducting tape are shown in Figure 1, as a function of bending strain, described by the parameter e, which is defined thus:

$$e\ (\%) = 100\ t/D \tag{1}$$

where t is the thickness of the tape, and D is the diameter of its bending.

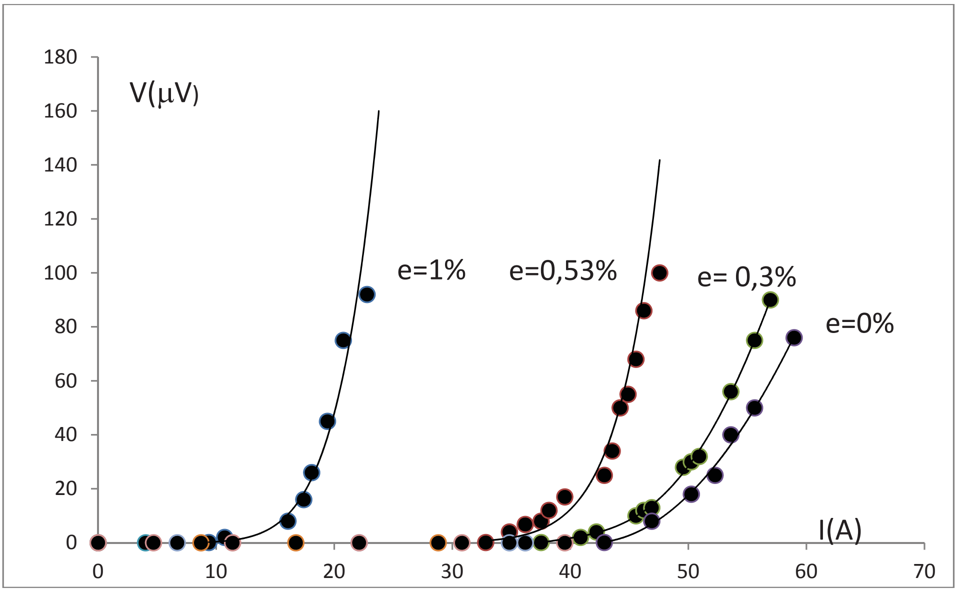

Fig. 1. Measured current-voltage characteristics of superconducting BiSrCaCuO tape at liquid nitrogen temperature, as a function of the bending strain given for each curve

The dots are experimental data, while the solid lines give polynomial or power law type approximations with a power exponent larger than six. This number characterizes the quality of the superconductor in a power law model. The results shown in Figure 1 clearly indicate the strong influence of the bending process on the current-voltage characteristics and critical current of HTc tape. This effect is shown directly in Figure 2.

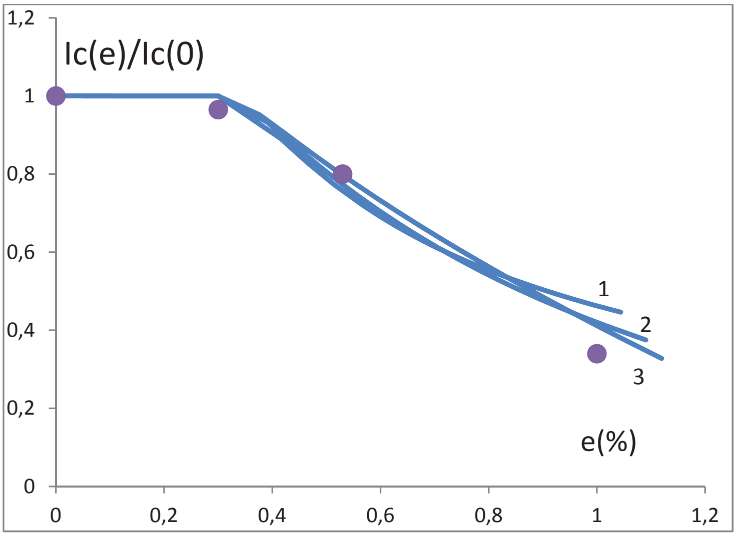

Fig. 2. The dependence of the critical current of the deformed BiSrCaCuO tape on the bending strain parameter e. The dots indicate experimental data, while the solid lines describe the rupture probability in: (1) fractional, (2) exponential and (3) linear approximation

2. PRESENTATION OF THE MODEL AND THE RESULTS OF CALCULATIONS

In the paper has been taken that shown in Figure 2 critical current dependence on the bending strain, given by parameter *e*, is described by the rupture probability $G(e)$ through the relation:

$$G(e) = 1 - I_c(e)/I_c(0) \tag{2}$$

Additionally, according to the experimental data shown in Figure 2, it has been admitted that for $e < e_c$ we have an elastic reversible region, in which micro-cracks do not appear, therefore $G(e < e_c) = 0$, where e_c is critical strain which does not yet lead to the formation of micro-cracks when applied to the superconducting tape.

Then basing on the experimental data shown in Figure 2 it has been approximated the rupture probability for $e > e_c$ by the linear, fractional and exponential functions according to the relations given below and shown in Figure 2. In above mentioned cases $G(e)$ is equal to:

$$G(e) = 0,96\,(e - e_c) \tag{3}$$

$$G(e) = 1 - \frac{1}{1,036 + 1,72(e - e_c)} \tag{4}$$

$$G(e) = 1 - \exp\left[1{,}4\left(e_c - e\right)\right] \tag{5}$$

Each of these approximations produced similar results, closely matching the experimental data. The change of the critical current in folded superconducting tape is connected with the creation of micro-cracks, it is regions in the superconductor of the smaller cross-section, so in this way of the higher transport electric current density. Then according to [4] we can treat the multi-filamentary superconducting tape as a long line containing un-deformed and deformed sections of the filaments, which additionally are joined parallel through the silver matrix to the sheath. A model describing such a configuration can be seen in Figure 3, which shows the elasticity coefficients in a filament deformed by the presence of regularly arranged micro-cracks, coupled to the sheath by the shear interaction with the matrix. k_{fil} is the spring constant of the filament, while e_{fil} is the strain on the filament, which, due to the amortizing effects in the silver matrix, is smaller than the applied bending strain e_{app}. Equivalent elasticity parameters describing the shearing interaction of the filament with the sheath, through the matrix noted as k_{sheath} and e_{sheath}, are also shown in Figure 3.

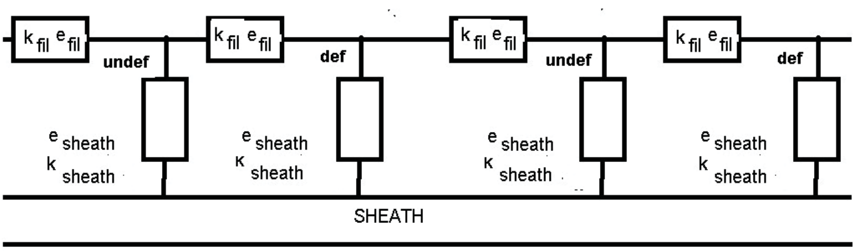

Fig. 3. Elasticity model of filamentary superconducting tape as a long line of ordered undeformed (undef) and deformed (def) regions

By way of analogy, as in [4], we can transform this picture, showing a mechanical model of the elasticity parameters of the HTc superconducting tape, into an equivalent electric model of a long line of resistors, as shown in Figure 4.

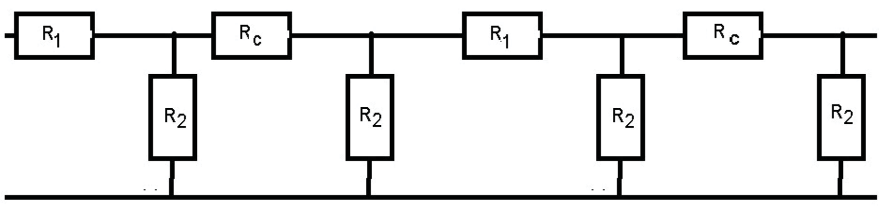

Fig. 4. Approximation of the deformed HTc superconducting filamentary tape through the long line of resistors joined in the row and parallel

In Figure 4, R_1 is the resistivity per unit length of the undeformed filament in its resistive state, which corresponds to the elasticity parameter k_{fil}, while $1/R_2$ is the appropriate conductivity of the matrix, which in this nomenclature corresponds to the elasticity constant k_{sheath} shown in Figure 3. R_c is the resistivity per unit length of the deformed filament with micro-cracks, in the resistive state. Basing on analysis of the Figure 4 it is easily to find then the simple mathematical relations describing variation with the depth inside the line of the voltage and current in such long line taking into account the leakage of the current through normal matrix and voltage drop. The relations $dV/dx = -R_1 I$ and $dI/dx = -V/R_2$ lead to the dependences:

$$\frac{d^2 I}{dx^2} = \frac{R_1}{R_2} I \qquad \frac{d^2 V}{dx^2} = \frac{R_1}{R_2} V \tag{6}$$

Falling solution of first from Equation 6 has been found in the exponential form:

$$I(x) = I(0)\exp\left(-\sqrt{\frac{R_1}{R_2}}x\right) \tag{7}$$

and then finally:

$$V(x) = I(0)\sqrt{R_1 R_2}\cdot\exp\left(-\sqrt{\frac{R_1}{R_2}}x\right) \tag{8}$$

while effective resistivity per unit length of the long line is:

$$R_{eff} = \sqrt{R_1 R_2} \tag{9}$$

By analogy the expression for the effective resistivity per unit length of the long line, containing deformed filaments joined in parallel to the sheath, is:

$$R_{efc} = \sqrt{R_c R_2} \tag{10}$$

Following from Figures 3 – 4 and according to [4], in this dual formalism relations between the strain parameters of the mechanical network and the resistivity of the equivalent electric long line arise:

$$\frac{e}{e_{fil}} = \frac{R_1}{R_{eff}} = \frac{k_{fil}}{k_{eff}}, \qquad \frac{R_2}{R_1} = \frac{k_{sheath}}{k_{fil}} \tag{11}$$

The above considerations should be supplemented with an additional condition to reflect the fact that if a micro-crack occurs, stress force will be directed onto the sheath. Therefore the elasticity properties of the sheath are attenuated, while coefficient k_{sheath} should decrease then with rupture probability $G(e)$. In the present paper this dependence has been proposed in the following form:

$$k_{sheath}(e) \sim k_{fil} \frac{1-G(e)}{1+G(e)} \tag{12}$$

Additionally we notice that although the same current flows through the superconducting tape of the cross-section *S*, others are current-voltage characteristics in undeformed and deformed through the existence of the micro-cracks regions, because current density is different then. This effect concerns resistivity R_1 and R_c describing the undeformed section of the tape and the deformed one, as follows from the next relations:

$$R_1 = E(\frac{I}{S})/I \qquad\qquad R_c = E(\frac{I}{S\nu(1-G)})/I \tag{13}$$

Here $E(j)$ is the dependence of the generated electric field on the transport current density, in other words the current-voltage characteristic. Assuming that the depth of the micro-crack is proportional to rupture probability *G*, we obtain the effective cross-section of the deformed tape as $S\nu(1\text{-}G)$. ν is the coefficient of proportionality, containing too the effect of non-total filling of the tape by the filaments.

Total resistivity of the superconducting tape per unit length is therefore the amount of both of these components with the appropriate weight:

$$R_{eff} = \sqrt{R_1(1-e+e_{fil})R_2} + \sqrt{R_c R_2(e-e_{fil})} \tag{14}$$

In Equation 14 it has been assumed that the length of the micro-crack, in other words the length of the deformed region, is in this model equal to the difference between the applied strain *e* and the strain e_{fil} acting on the filament, which are according to Equations 9-12 joined by the proportionality relation:

$$e \sim \sqrt{\frac{1+G(e)}{1-G(e)}}\; e_{fil} \tag{15}$$

The current-voltage characteristics appearing in Equation 13 of the HTc layered superconductor have been determined, taking into account the model of the interaction of the pancake type vortices created in HTc superconductors with flat defects [5] like the micro-cracks considered in the present work. A view of the captured vortex on a rectangular nano-sized defect for this geometry is shown in Figure 5, while the meanings of the symbols used here are given below:

$$S_1 = \xi^2 \arcsin\frac{d}{2\xi} \qquad S_2 = \frac{d}{2}\sqrt{\xi^2 - \frac{d^2}{4}} \qquad \alpha = 2\arcsin\frac{d}{2\xi} \tag{16}$$

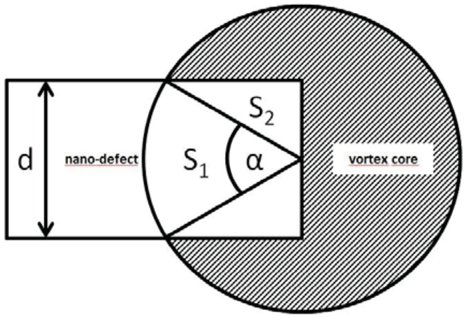

Fig. 5. Scheme of the initial configuration of a pancake vortex captured by a nano-sized defect. The symbols are explained in the text

Deflection of the vortex on the distance x_m leads to the enhancement of the energy of the system balanced by the Lorentz force potential. An energy barrier appears, whose maximum is given as:

$$\Delta U\left(x_m\right)=\frac{\mu_0 H_c^2}{2} l \xi^2\left(\arcsin\left(\frac{x_m}{\xi}\right)-\frac{\pi}{2}+\arcsin\left(\frac{d}{2\xi}\right)+\frac{x_m}{\xi}\sqrt{1-\left(\frac{x_m}{\xi}\right)^2}+\frac{d}{2\xi}\sqrt{1-\left(\frac{d}{2\xi}\right)^2}\right)-jB\pi\xi^2 l x_m \tag{17}$$

H_c is the thermodynamic critical magnetic field, l is the thickness of the superconducting layer, d the width of the pinning centre, ξ the coherence length. Next we write equation 17 applying the relation connecting the position of the maximum of the energy barrier x_m with the reduced current density $i = j/j_c$:

$$x_m=\xi\sqrt{1-i^2} \tag{18}$$

Then we obtain a new form of potential barrier already dependent on the reduced current density i:

$$\Delta U\left(i\right)=\frac{\mu_0 H_c^2}{2} l \xi^2\left(-\arcsin(i)+\arcsin\left(\frac{d}{2\xi}\right)+\frac{d}{2\xi}\sqrt{1-\left(\frac{d}{2\xi}\right)^2}-i\sqrt{1-i^2}\right) \tag{19}$$

In the case of large micro-cracks, starting from the condition $d = 2\xi$, relation 19 can be reduced to this form, which has been used finally in the present paper:

$$\Delta U\left(i\right)=\frac{\mu_0 H_c^2}{2} l \xi^2\left(-\arcsin\left(i\right)+\frac{\pi}{2}-i\sqrt{1-i^2}\right) \tag{20}$$

Equation 20 satisfies the required condition of a positive value of the potential barrier for electric current smaller than critical and vanishing potential barrier for critical current density. The potential barrier determines the probability of the flux creep process, in which an individual pancake vortex transporting magnetic flux is moved during electric current flow, so the current-voltage characteristic is determined in this way. Examples of calculations made of the current-voltage characteristics as a function of bending strain are shown in Figure 6 and indicate qualitatively good agreement with the experimental data shown in Figure 1.

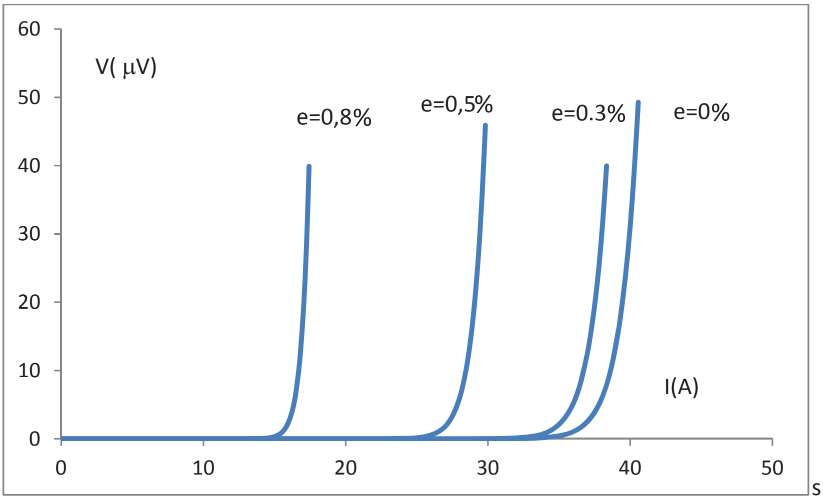

Fig. 6. Influence of the bending strain *e* on the theoretical current-voltage characteristics of the deformed superconducting tape

Figure 7 on the other hand shows the influence of the form of the rupture probability described by function *G* on the current-voltage characteristics. For the various considered shapes of the function describing the rupture probability, the current-voltage characteristics are similar.

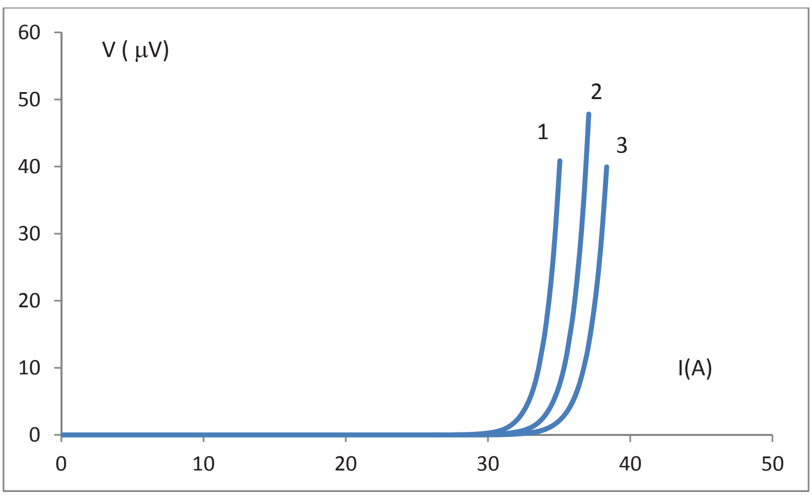

Fig. 7. Influence of the shape of rupture probability *G*(*e*) on the current-voltage characteristics for function *G* described by (1) Eq. 4, (2) Eq. 5 (3) Eq. 3

3. CONCLUSIONS

The above analysis shows the importance of the influence of bending strain on the current-voltage characteristics and critical current of HTc multifilamentary superconducting tapes. Measurements of the current-voltage characteristics in folded tape, performed on first generation superconducting tape, are in qualitative agreement with the theoretical approach.

LITERATURE

1. Sosnowski J.: Superconducting cryocables. Book Publisher of Electrotechnical Institute, in Polish, pp. 1-100, 2012.
2. Sosnowski J.: Superconducting cables – analysis of operation and applications in electric grids. Proceedings of the Electrotechnical Institute, vol. LXIII, issue 274, pp. 89-96, 2016.
3. Drozdov A.P., Eremets M.I., Troyan I.A., Ksenofontov V., Shylin S.I.: Conventional superconductivity at 203 kelvin at high pressures in the sulfur hydride system. Nature Letter vol. 525, pp. 73–76, 2015.
4. Kiss T. et al: Transport Properties of Multifilamentary Ag-Sheathed Bi-2223 Tapes under the Influence of Strain, IEEE Trans. on applied superconductivity, vol. 11, issue 1, pp. 3888-3891, 2001.
5. Sosnowski J.: New model of the pinning potential barrier in layered HTc superconductors. Mod. Phys. Lett. B, vol. 30, no. 31, pp. 1650387-1 – 1650387-17, 2016.

Accepted for publication 28.04.2017

ANALIZA WPŁYWU ODKSZTAŁCENIA POWSTAŁEGO PRZY ZGINANIU NA CHARAKTERYSTYKI PRĄDOWO-NAPIĘCIOWE WYSOKOTEMPERATUROWYCH TAŚM NADPRZEWODZĄCYCH

Jacek SOSNOWSKI

STRESZCZENIE *W artykule zbadano wpływ naprężenia i odkształcenia powstałego podczas zginania wysokotemperaturowych taśm nadprzewodnikowych, szczególnie podczas nawijania elektromagnesów nadprzewodnikowych na ich charakterystyki prądowo-napięciowe i prąd krytyczny. Przedstawiono model teoretyczny, który jakościowo opisuje wyniki badań doświadczalnych przeprowadzonych na taśmach nadprzewodnikowych I generacji. Zbadano wpływ funkcji określającej prawdopodobieństwo występowania mikropęknięcia na charakterystyki prądowo-napięciowe i prąd krytyczny.*

Słowa kluczowe: *wysokotemperaturowe taśmy nadprzewodnikowe, odkształcenie przy zginaniu, charakterystyki prądowo-napięciowe*